



Thermal expansion and mechanical properties of urethane-modified epoxy bonded CFRP/steel joints at low and high temperatures for automotive

Kyeng-Bo Sim^a, Tae-Hyung Lee^a, Gi-Yeon Han^a, Hyun-Joong Kim^{a,b,*}

^a Laboratory of Adhesion and Bio-Composites, Department of Agriculture, Forestry and Bioresources, College of Agriculture and Life Sciences, Seoul National University, Seoul 08826, Korea

^b Research Institute of Agriculture and Life Sciences, College of Agriculture and Life Sciences, Seoul National University, Seoul 08826, Korea

ARTICLE INFO

Keywords:

Urethane modified epoxy
Epoxy
CTE mismatch
Internal stress
Reliability

ABSTRACT

Long-term reliability is critical in automobiles owing to their frequent exposure to the external environment and lengthy operational durations. Using dissimilar materials as adhesives to reduce the weight of vehicles results in a mismatch of coefficients of thermal expansion (CTE). Difference in CTE causes constant internal stress at the adhesive interface when the temperature changes, leading to delamination of the adhesive at the interfaces, microcrack initiations, and crack propagations. Therefore, a blend of linear urethane prepolymer and epoxy was tested to alleviate stress concentration. Dynamic mechanical analysis (DMA) was performed to determine the modulus according to the urethane content, while tensile strength was measured to evaluate changes in the physical properties. It was observed that increasing the urethane content decreased the modulus but progressively enhanced the tensile strength elongation rate. The lap shear strength specimen was thermally shocked to validate the decrease relative to the initial value based on the cycles. Consequently, combining urethane and epoxy successfully enhanced the elongation and reduced the internal stress caused by temperature changes.

1. Introduction

Epoxy adhesives are among the most often used thermosetting polymers owing to their excellent mechanical qualities. Epoxies possess amorphous structures and high cross-linking densities, while exhibiting high modulus and low creep characteristics [1–3]. As a result of its high adhesive strength, thermal stability, and chemical resistance, it is used in a wide variety of applications, including automotive, aerospace, marine industries, and electronics [4–7]. However, the highly cross-linked structure renders them brittle, and the materials exhibit poor resistance toward crack propagation [8,9]. This brittleness is significantly affected by the temperature variations, particularly after bonding with various materials for weight reduction [1,3].

In the current automotive industry, lightweight design is a crucial component. Owing to the decreasing fuel efficiency due to the weight of batteries in electric cars, weight reduction of materials is becoming increasingly essential. In addition, carbon dioxide emission regulations are progressively being tightened, lowering the usage of steel and boosting the use of various lightweight materials—carbon-fiber-reinforced plastics (CFRP) and aluminum (AL). All materials have varying

coefficients of thermal expansion (CTEs) with varying temperature [10]. Under temperature fluctuations, each material experiences differential thermal shrinkage and expansion. Particularly, organic materials tend to possess higher CTEs compared to inorganic materials. However, CTE mismatch becomes a challenge while bonding epoxy materials with other substances [11–14].

Automotives are frequently affected by temperature variations, and the current issue of CTE mismatch poses challenges to long-term reliability [15,16]. When subjected to continuous thermal cycling, internal stress is received at the adhesive interfaces as different materials, such as steel and CFRP, cannot follow the substantial expansion and contraction variations of the adhesive. When this internal stress continues to persist, issues such as peeling and cracking occur [14,17]. When subjected to continuous internal stress due to temperature changes, in the case of neat epoxy, the initiation and propagation of microcracks occur. When such a propagation occurs, delamination occurs at the adhesive interface, eventually creating a concern in long-term reliability [18–20].

To relieve the internal stress caused by CTE mismatch, it is necessary to control the epoxy that expands and contracts the most. The first approach is to lower the CTE. Usually, inorganic fillers with low CTEs

* Corresponding author at: Laboratory of Adhesion and Bio-Composites, Department of Agriculture, Forestry and Bioresources, College of Agriculture and Life Sciences, Seoul National University, Seoul 08826, Korea.

E-mail address: hjokim@snu.ac.kr (H.-J. Kim).

<https://doi.org/10.1016/j.compstruct.2023.117426>

Received 9 January 2023; Received in revised form 23 June 2023; Accepted 2 August 2023

Available online 3 August 2023

0263-8223/© 2023 Elsevier Ltd. All rights reserved.

(nano clay, nano silica) are used to lower CTE [11,12,21,22]. The second approach focuses on controlling the thermal expansion rate by increasing the crosslinking density and minimizing molecular movement. However, a higher degree of crosslinking can make the epoxy more brittle than before, potentially compromising its toughness and impact resistance [23,24]. Mechanical qualities are critical when it comes to the application of epoxy in automobiles. The modification of epoxy can be the final approach. By incorporating additives, such as liquid rubber or core shell rubber particles, into the neat epoxy formulation, the internal stress can be dispersed and crack resistance can be strengthened [23,25–27]. In certain cases, a low modulus component (urethane-modified epoxy) material is added and blended. The brittle properties can be reinforced by increasing the elongation and flexibility of the epoxy having a high modulus [28]. It is highly effective in alleviating the internal stress concentration because of its ability to change freely during temperature variations owing to the aforementioned elongation feature and increased flexibility [29,30].

Most previous studies have predominantly focused on lowering the CTE using inorganic fillers to resolve the CTE mismatch issue. Although the method is effective in the case of semiconductors, it presents several limitations in the automotive field, where impact resistance, strength, and vibration resistance are crucial requirements.

In this study, the usage of urethane-modified epoxy to mitigate the stress concentration issue induced by CTE mismatch was investigated. Epoxy, having a cross-linked network structure, and a linear urethane prepolymer were used together to form a semi-interpenetrating polymer network (IPN) structure after curing. While retaining the epoxy's excellent adhesiveness, the brittleness was supplemented by the linear urethane prepolymer through the aforementioned combination, which additionally improved the flexibility and elongation. To confirm whether the internal stress was relieved through the elongation characteristics, lap shear strength samples were made, and a thermal shock test was conducted. The test was repeated for 0, 24, 48, and 72 cycles, and the decrease in lap shear strength compared to the initial value was confirmed. Fracture shapes were observed after the thermal shock, allowing for the identification of locations with internal stress and any changes that happened as the cycles continued.

2. Materials and methods

2.1. Material

The epoxy YD-128 was derived from bisphenol A diglycidyl ether (DGEBA, Kukdo Chemical), having an epoxide equivalent weight (EEW) of 184–190 (g/eq), which was used in the present study. UME-330 was a linear urethane prepolymer-modified liquid epoxy resin. An EEW of 265–280 (g/eq) was utilized for flexibility and elongation. Dicyandiamide (Dyhard100s, Alzchem) and 3,3'-(4-methyl-1,3-phenylene) bis(1,1-dimethylurea) (Dyhard UR500, Alzchem) were used as the curing agent and accelerator (Table 1). The epoxy and curing agent were used in a 1:1 equivalent ratio. The accelerator was used at 1 phr to adjust the

Table 1
Components of adhesives.

Material	Composition	Equivalent (g/eq)	Form
YD-128 (Kukdo)	Bisphenol A diglycidyl ether	187	Liquid
UME-330 (Kukdo)	Urethane prepolymer modified liquid epoxy resin	272.5	Liquid
Dyhard 100 s (Alzchem)	Dicyandiamide	21	Powder
Dyhard UR500 (Alzchem)	3,3'-(4-methyl-1,3-phenylene) bis (1,1-dimethylurea)	3	Powder

curing temperature and time.

2.2. Specimens

The specimens utilized in this study included a steel plate (CR340) and an autoclave carbon fiber-reinforced polymer (CFRP). The CFRP was fabricated by laminating in $[0^\circ/90^\circ]$ 13 plain-weave prepreps (WSN-3KT, 100 mm \times 25 mm \times 2.5 mm, SK Chemicals). The steel plate employed was cold rolled steel (CR340, 100 mm \times 25 mm \times 1.6 mm, Posco Chemical Co., Ltd.), a commonly used material in automobiles. All specimens were subjected to cleaning through sonication for 10 min with alcohol, followed by natural drying for 20 min before testing.

2.3. Preparation of urethane-modified epoxy (UME)

Two materials UME-330 and YD-128 were used for blending the urethane-modified epoxy. UME-330 contains 30% linear urethane prepolymer and 70% DGEBA. Experiments were carried out with 0, 10, 15, 20, 25, and 30 wt% of linear urethane prepolymer obtained by diluting UME-330 in DGEBA (UME0, UME10, UME20, UME25, UME30). Table 2 shows the details of the composition of the urethane-modified epoxy blend.

2.4. Dynamic mechanical analysis (DMA)

DMA (Q800, TA Instruments) was used to assess the modulus and tan Delta behavior according to UME content. For 0–30% UME content, rectangular specimens were prepared using a silicone molder.

(80 mm \times 10 mm \times 4 mm). The measurement was conducted using a dual cantilever at 0.1% strain under 1 Hz frequency (under ASTM D5418) in the temperature range of -55°C to 200°C at a constant heating rate of $5^\circ\text{C}/\text{min}$.

2.5. Thermomechanical analysis (TMA)

A linear change according to the UME content was investigated based on the temperature using a thermomechanical analyzer (TMA (Q400), TA Instrument). Samples were scanned under a nitrogen atmosphere from room temperature to 200°C at a heating rate of $5^\circ\text{C}/\text{min}$.

2.6. Tensile test

As the UME content was increased, the variations in the stress, strain, and elongation were determined at low (-55°C), high (125°C), and room temperature, and the values were compared with those for the conventional DGEBA (under ISO 527–2). The test was conducted on a universal testing machine (UTM Z010, Zwick) in a temperature-controlled chamber.

Samples were produced in a silicone mold while following the ISO-527 standards. For curing, the silicone mold was preheated at 160°C for 30 min; the prepared material was injected into the silicone mold and cured at 160°C for 30 min in a vacuum oven. The prepared specimens were stored in a room at constant temperature and humidity for 1 h, and

Table 2
Composition of urethane-modified epoxy blend.

Sample	YD-128 (g)	UME-330 (g)	Equivalent (g/eq)	Dyhard 100 s (g)	Dyhard UR500 (g)
0	100	0	187	11.23	1
10	66.67	33.33	208.84	10.06	1
15	50	50	221.8	9.47	1
20	33.33	66.67	236.46	8.89	1
25	16.67	83.33	253.2	8.29	1
30	0	100	272.5	7.7	1

then placed in the chamber to conduct the experiment. Measurements were obtained under three conditions ($-55\text{ }^{\circ}\text{C}$, room temperature, and $125\text{ }^{\circ}\text{C}$). Before measurement at each temperature, the chamber was maintained at the respective temperature for approximately 1 h.

2.7. Single-lap shear test

The blended adhesive was applied to the steel plate (CR340) and autoclave CFRP. The bonding area was adjusted by using a spacer of $12.5\text{ mm} \times 25\text{ mm}$ and 0.18-mm-thick Teflon tape (AGF-100FR, Chukoh Chemical Industries). After curing at $160\text{ }^{\circ}\text{C}$ for 30 min, the bonded sample was stored in a room at a constant temperature and humidity for approximately 1 h. The thermal shock test was conducted for 0, 24, 48, and 72 cycles, and after each cycle, the measurement was acquired after storage at $23\text{ }^{\circ}\text{C}$ and 55% relative humidity for an hour. The change in shear stress after each thermal cycle was compared with the initial value. The experiment was conducted at the speed of 5 mm/min on the UTM. After repeating the cycle, the decrease in lap shear strength compared to the initial value was confirmed.

$$\text{Decreased Rate (\%)} = \frac{\tau_{\text{cycle}0} - \tau_{\text{cycle}72}}{\tau_{\text{cycle}0}} \times 100$$

The decreased rate indicates the decrease in rate after 72 cycles thermal shock compared to the initial value. $\tau_{\text{cycle}0}$ denotes the lap shear strength measured without thermal shock and $\tau_{\text{cycle}72}$ indicates the lap shear strength after 72 cycles of thermal shocking.

2.8. Thermal shock test

Thermal shock test was conducted to assess the impact of CTE mismatch-induced internal stress at repeating cycles of low and high temperatures. It was primarily used to evaluate the long-term reliability of the specimens and identify potential causes of failure.

The test was conducted using the TSA-40L-A Expec (Japan) equipment according to the shock conditions specified in the MIL-STD-883 standard, which are more stringent than the conditions applied in general automobile reliability evaluation tests. The tests were performed in the temperature range of $-55\text{ }^{\circ}\text{C}$ to $125\text{ }^{\circ}\text{C}$ and in multiple cycles (0, 24, 48, 72 cycles), with each cycle encompassing two steps—the first step conducted at $125\text{ }^{\circ}\text{C}$ for 30 min and the second step conducted at $-55\text{ }^{\circ}\text{C}$ for 30 min. The dwelling time between the two steps was approximately 10 min at room temperature.

3. Results and discussion

3.1. Structural characteristics of blended materials

Two types of adhesives DGEBA epoxy adhesive and linear urethane prepolymer were blended to offset the disadvantages of each when used alone. Conventional epoxy exhibits high strength; however, it is limited by its inherent brittleness and low elongation properties [18–20]. In contrast, the urethane adhesive demonstrates flexible characteristics and high elongation but possesses lower strength due to its soft material

characteristics.

We used the two aforementioned materials to compensate for each other's shortcomings. As the epoxy is cross-linked to the linear urethane prepolymer, a semi-IPN structure is formed, as shown in Fig. 1. Thus, the ratio of the DGEBA and linear urethane prepolymer contents can be adjusted to control the flexibility and rigidity of the adhesive. The resulting chain structure improves the brittleness and flexibility of DGEBA. Owing to the improved flexibility, the problem of stress concentration can be solved by redistribution of the stress [31].

3.2. Dynamic mechanical analysis

The DMA results show the storage modulus and glass transition according to the DGEBA and urethane prepolymer contents. In the case of the temperature range, the temperature was increased from $-50\text{ }^{\circ}\text{C}$ to $275\text{ }^{\circ}\text{C}$. This was done to determine whether phase separation occurred in the tan Delta to confirm the successful blending of the two materials [32,33]. It was confirmed that one peak appeared up to $275\text{ }^{\circ}\text{C}$. Fig. 2 (a) shows that the storage modulus gradually decreases as the UME content increases, which is attributed to the softness of the latter. Fig. 2 (b) shows the glass transition temperature. The maximum value of tan Delta represents the value of the glass transition. In the case of neat epoxy, the glass transition temperature (T_g) was $160\text{ }^{\circ}\text{C}$, and no significant change was observed with increase in the linear urethane prepolymer content. Depending on the content, T_g values of 161, 161, 160, 160, 159, and $158\text{ }^{\circ}\text{C}$ were observed. The high temperature of $125\text{ }^{\circ}\text{C}$ in the thermal shock test did not appear to influence the T_g .

3.3. Thermal expansion of substrates and adhesives

A mismatch in the CTE occurs when different materials are bonded; this CTE mismatch between dissimilar materials is a critical factor that often leads to reliability issues when they are bonded together [11–14]. Different expansions and contractions occur when the temperature varies, and the material that expands the most experiences the most internal stress. As different materials expand forcibly without being able to keep up with the large expansion, this internal stress acts at the interface where the materials are bonded.

Based on the TMA data presented in Fig. 3, the difference in expansion in the case of dissimilar materials and adhesives was observed to be more than sixfold. This observation indicates that the adhesive undergoes the largest expansion and contraction as the temperature changes. In the case of adhesion between dissimilar materials, a significant amount of internal stress is generated at the interface under repeated expansions and contractions. Neat epoxy is brittle because of its high crosslinking density, resulting in microcracks when the thermal cycle is repeated [34,35]. Therefore, it is important to use it in conjunction with a linear urethane prepolymer to enhance flexibility and alleviate stress concentration during expansion and contraction. In the case of conventional rigid neat epoxies, stress concentration occurs severely during expansion and contraction due to the high modulus during expansion. As the UME content between the molecules increases, the density of the network structure decreases and CTE increases (Fig. 3

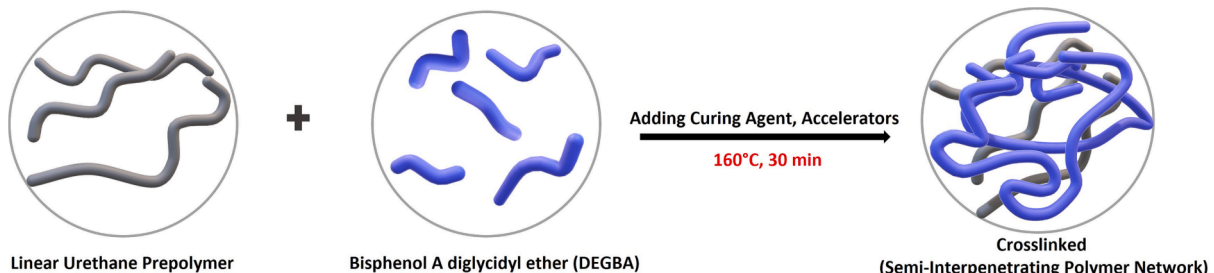


Fig. 1. Schematic of semi-IPN structure of UME.

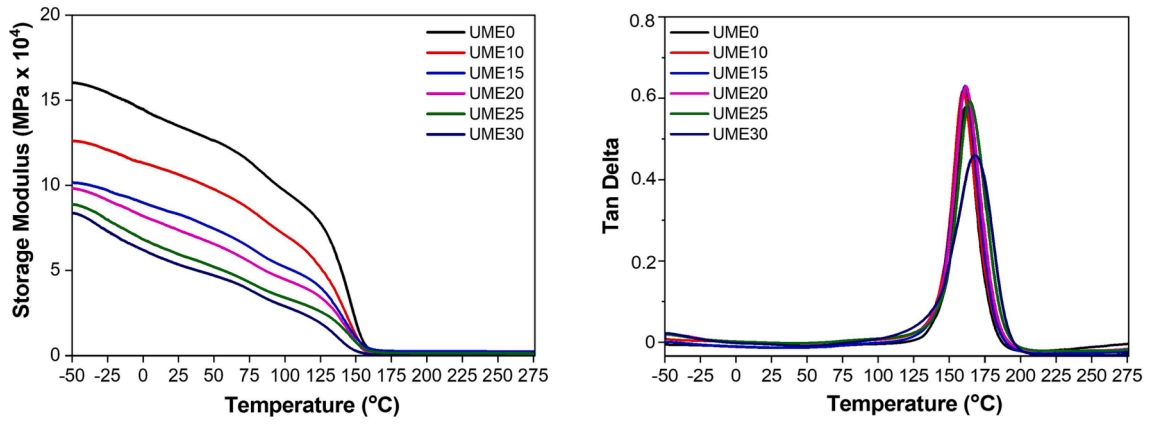


Fig. 2. (a) Storage modulus of DGEBA/UME; (b) Tan Delta of DGEBA/UME.

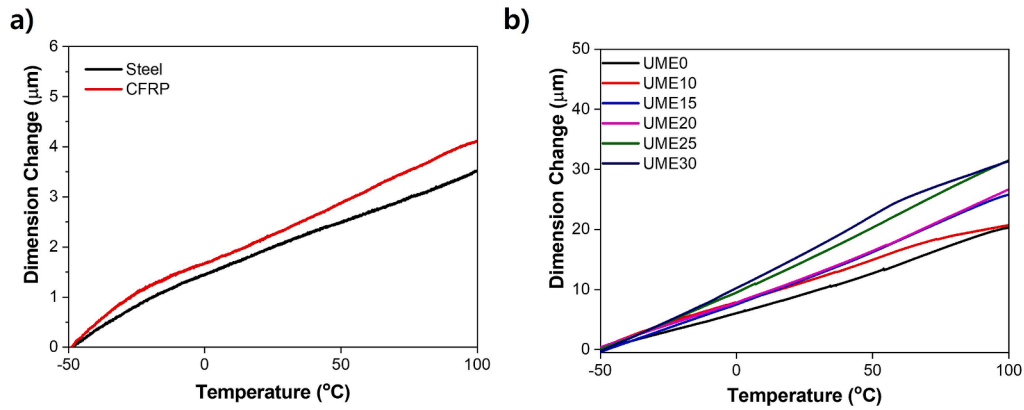


Fig. 3. TMA data: (a) Change in dimension of CFRP and steel; (b) Change in dimension with UME content.

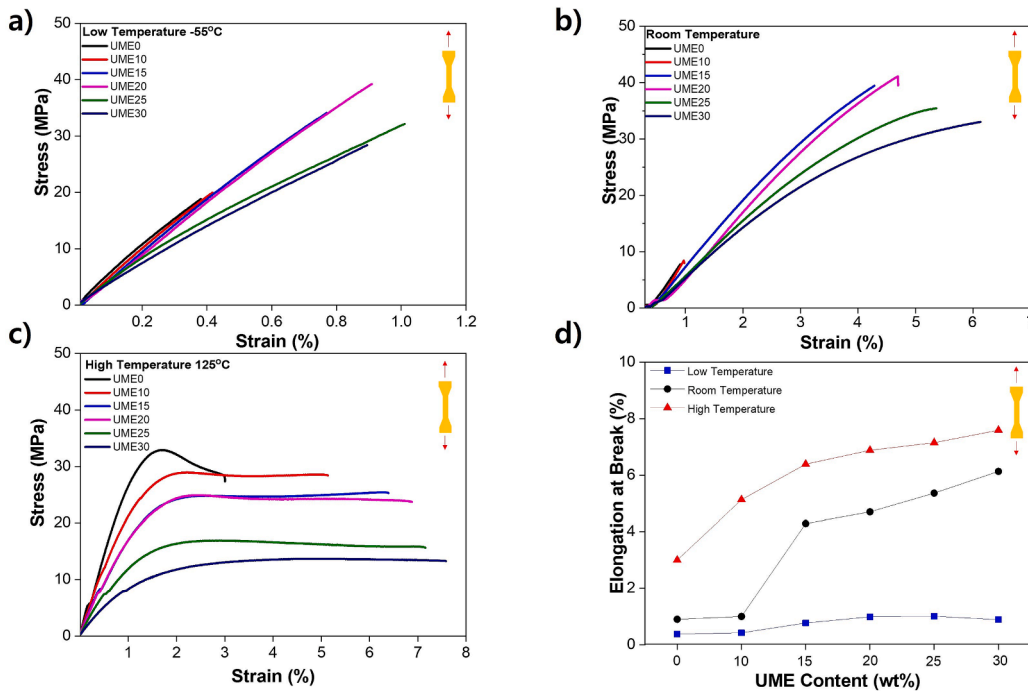


Fig. 4. Stress-strain curves at (a) Room temperature, (b) High temperature, and (c) Low temperature; (d) Elongation at break for various UME contents and temperatures.

(a), (b)).

3.4. Temperature effects on stress–strain curve for different UME contents

To confirm the change in behavior according to the temperature variations, dog-bone shaped samples of the adhesive were prepared, and the tensile strength was measured using the UTM. An experiment was conducted to confirm the strain–stress results of the adhesive according to the temperature change. Regarding the thermal shock temperature, a cycle test was conducted at a low temperature of $-55\text{ }^{\circ}\text{C}$ and high temperature of $125\text{ }^{\circ}\text{C}$ to confirm the change in adhesive properties at this temperature.

Specimens were prepared with a UME content of 10–30 wt%. As the urethane content increases, the rigidity decreases and flexibility improves (Fig. 4 (a), (b), (c)). It can be observed that UME0 exhibits considerably less elongation within the range of the room temperature. The particularly low strain at break is due to the properties of the neat epoxy (Fig. 4 (d)); owing to its high crosslinking density, the epoxy possesses rigid yet brittle properties, and even a minor impact can induce breaking.

The results show that the semi-IPN structure obtained by curing neat epoxy on the linear urethane prepolymer improves its brittleness and flexibility. At a low temperature of $-55\text{ }^{\circ}\text{C}$, extremely limited elongation is observed. Even when the urethane prepolymer content is increased, the maximum strain shows an elongation of less than 1%. As the temperature reduces, the adhesive shrinks, causing the molecules to come closer, which results in a high modulus [36–39]. The neat epoxy also possesses a high modulus; however, its brittle properties are enhanced at low temperatures. Thus, it could get damaged even under a small force. At a high temperature of $125\text{ }^{\circ}\text{C}$, significantly high elongation is observed. As the temperature increases, the adhesive expands and the molecules move away from each other, resulting in a low

modulus. The neat epoxy also exhibits an elongation of 3% or more [40,41].

The strain–stress results according to the temperature range indicate the lowest elongation at a low temperature. This is likely to have the greatest effect if the internal stress accumulates in the low-temperature region when expansion and contraction are repeated after bonding the dissimilar materials. In the case of UME0 and UME10 with low urethane content, the results of the strain at break showed that the elastic area is considerably small. That is, when stress occurs under repeated expansion and contraction, reliability issues such as microcracks may occur.

3.5. Adhesion performance of urethane-modified epoxy adhesive after thermal shock cycle test

After bonding the different materials (CFRP/steel) with the adhesive, a lap shear test was performed to examine the behavior of the changes according to the urethane content under cyclic thermal shock. As the urethane content increased, the lap shear strength increased. The brittle properties of neat epoxy appeared to be improved by the linear urethane prepolymer, and the improved toughness influenced the lap shear strength, which was recorded as 14, 17, 26, 32, 23, and 17 MPa for urethane contents of 0, 10, 15, 20, 25, and 30 wt%, respectively (Fig. 5 (a)). After 25 wt% of UME, the lap shear strength seemed to decrease with the decreasing internal cohesiveness [42].

The conditions of the thermal shock cycle were repeated for 0, 24, 48, and 72 cycles. Each cycle proceeded in the order of low temperature, room temperature, and high temperature, and a total of 72 cycles were conducted. As the thermal shock was repeated after bonding the dissimilar surfaces, the rate of reduction in the lap shear strength when compared with the initial value was determined. Fig. 5(c) shows that when the cycle is repeated, expansion and contraction according to high and low temperatures occur, resulting in a difference in the thermal

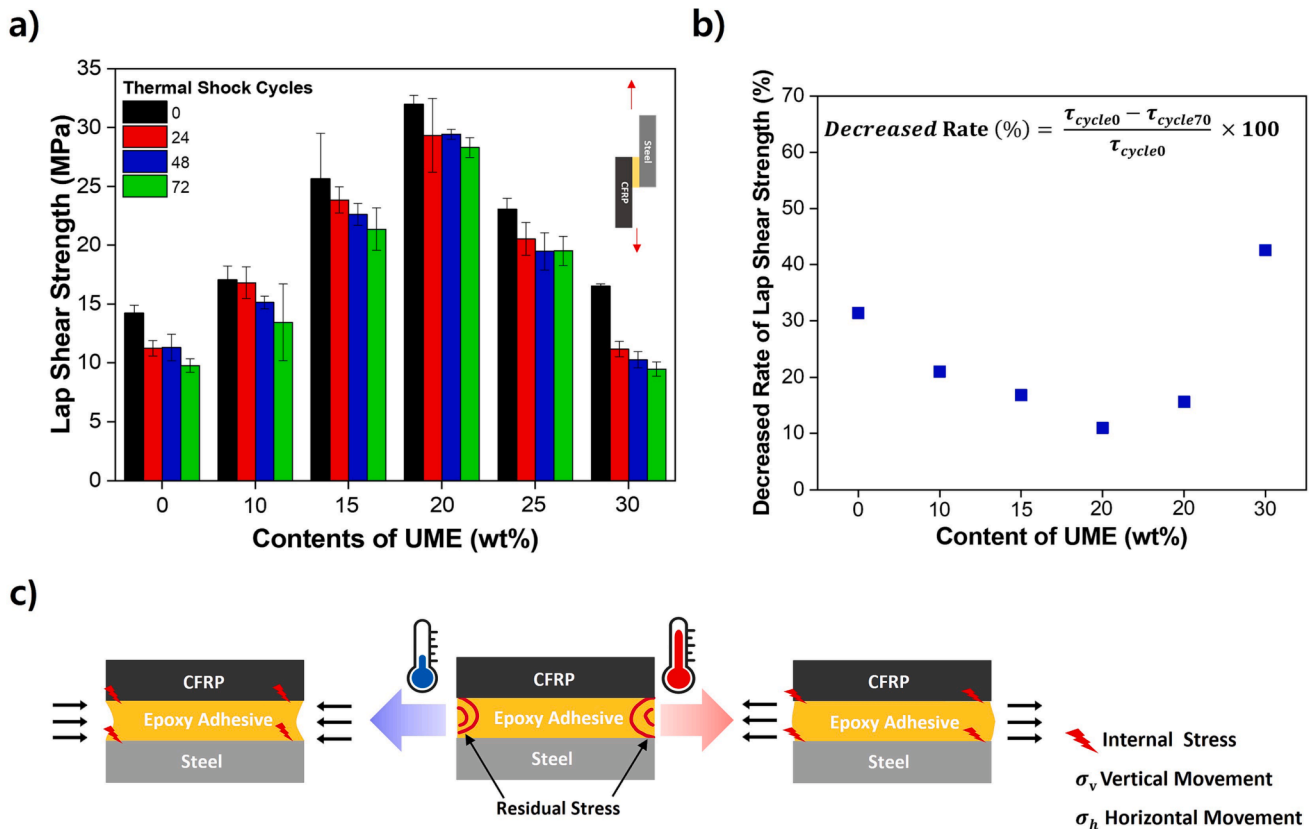


Fig. 5. (a) Lap shear strength according to thermal shock cycle; (b) Decreased rate of 72 cycles compared to initial value; (c) Schematic image of expansion and contraction according to temperature change in the adhesion of dissimilar materials.

expansion. Adhesives with higher rigidity experience greater internal stress during expansion and contraction, which causes significant defects such as delamination, crack initiation, or crack propagation. When the linear urethane content is increased, the elongation property of the adhesive is improved, resulting in better stress dispersion. This enhancement occurs because the adhesive is able to change easily when it expands and contracts [41].

After 72 cycles, the lap shear strengths decreased by -31%, -21%, -17%, -11%, -16%, and -43% from the initial values as follows. UME20 showed the highest lap shear strength and the smallest decrease when compared with the initial value. As the UME content increased, it showed effective results in relieving internal stress caused due to CTE mismatch. However, with increasing UME content, the softness increased and the lap shear strength value, compared to the initial value, gradually increased with the UME20 content.

3.6. Observation of adhesion fracture shape after lap shear test

The part that receives the greatest amount of thermal stress during thermal expansion and contraction is the interface. Because the adhesive and adherend are fixed at the interface, continuous thermal stress is generated at the interface during expansion and contraction. As shown in Fig. 6(a), when high and low temperatures are repeatedly applied, large expansion and contraction occur in the adhesive with a large CTE. When the adhesive undergoes thermal expansion and contraction, it can move in the vertical and horizontal directions. The expansion and contraction of the adhesive in the vertical direction can proceed freely without restrictions. However, the movement of the adhesive is limited in the horizontal direction. This is because the adherend and adhesive adhere to the interface, and when expansion and contraction occur, internal stress is concentrated due to the movement at the interface. If this internal stress is repeated, it affects the interfacial adhesion between the adhesive and adherend, resulting in microcracks or crack

propagation inside the adhesive [30,37].

As shown in Fig. 6(b), the adhesive shrinks at low temperatures. During this process, it is bonded to the adherend and tensile stress develops inside it. At high temperatures, the adhesive expands. During this process, the adherend and adhesive are bonded and compressive stress develops inside the adhesive. The modulus of UME0 and UME10 are large and rigid. Owing to their rigid properties, when low and high temperatures are repeatedly applied, a larger amount of stress is developed during contraction and expansion. Further, the samples have brittle characteristics, which cause defects (such as microcracks) under repeated internal stress. In the cases of UME15, UME20, UME25, and UME30, the stress-strain curve in the tensile stress results shows that the elastic region is significantly increased. This increase in the elastic area ensures flexibility during expansion and contraction to relieve the internal stress.

Fig. 6(c) shows the fracture shapes after the lap shear test. In this stage, the lap shear strength decreased the most when compared with the initial value, especially in the case of the samples in which interfacial fracture occurred. This implies that the initial bonding force between the interface and adhesive is weak in the case of the samples where interfacial failure occurs. In the case of the samples having weak bonding strength at the interface, the bonding strength further decreases when exposed to high and low temperatures owing to the internal stress that is continuously received at the interface. Therefore, UME0 and UME30 exhibited the most significant reduction in bonding strength. UME30 displayed the highest increase. It exhibited a higher decrease in internal cohesion within the epoxy adhesive because of softness compared to the neat epoxy. Conversely, UME10 demonstrates brittle characteristics due to its high modulus; therefore, it is susceptible to breakage even with minor impacts. Moreover, the interfacial bonding weakens with repeated cycles, thereby increasing the reduction width. Meanwhile, UME30, with its low internal cohesive force, exhibits partial failure rather than complete interfacial failure [42] (Fig S2).

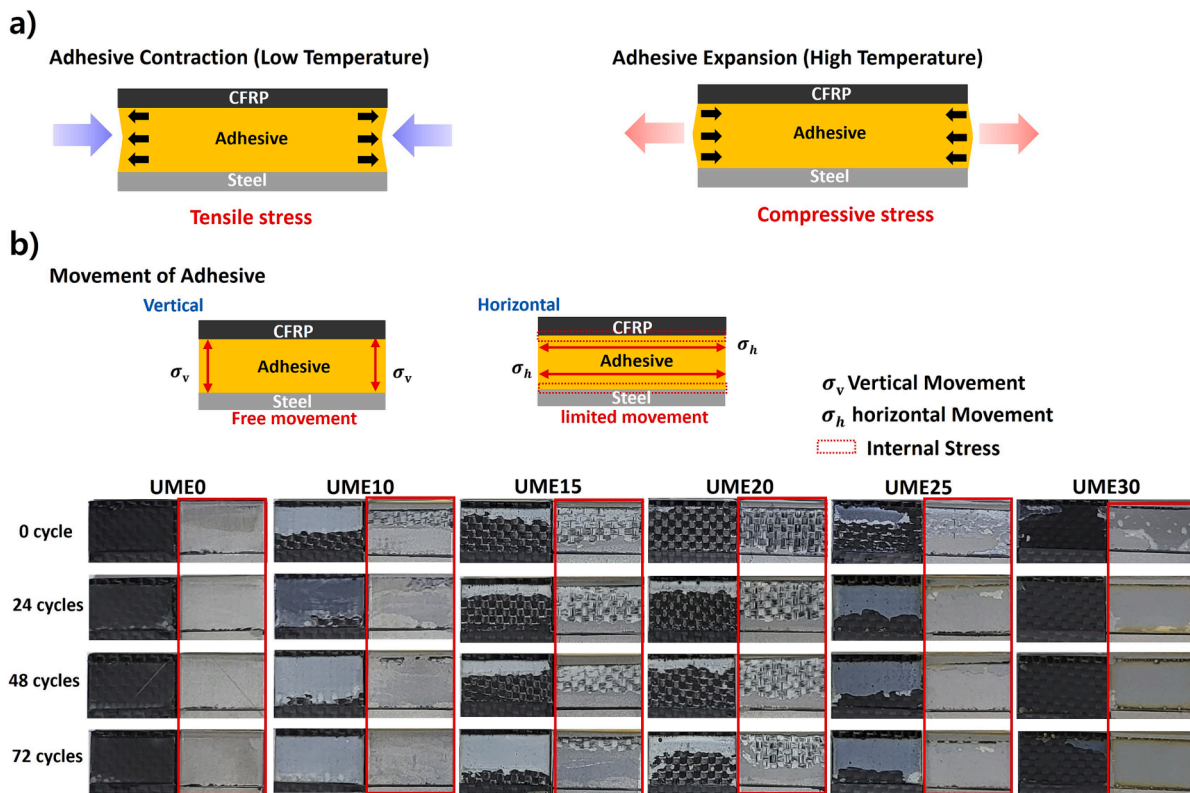


Fig. 6. (a) Direction of stress on the adhesive at low and high temperature; (b) Effect on internal stress of adhesive moving horizontally and vertically and fracture shape of the lap shear test after thermal cycle.

UME15, UME20, and UME25 not only exhibited the largest mixed-mode fracture, the smallest reduction in bonding strength was also noted in these. Thus, based on the fracture shape, it can be confirmed that interfacial adhesion is crucial when bonding dissimilar materials. The fracture shape changes over 0, 24, 48, and 72 cycles because the interfacial bond is weakened due to the constant internal stress at the interface.

4. Conclusion

In this study, a semi-IPN structure was created by blending a linear urethane prepolymer with neat epoxy to adjust the flexibility and elongation properties of the epoxy, while retaining its rigidity. From the tensile test results, it was confirmed that the elongation and elastic area increased as the UME content increased. This is vital not only for relieving internal stress caused by CTE mismatch, but also for enhancing impact resistance and mechanical properties. The thermal shock test conducted for 0, 24, 48, and 72 cycles demonstrated that as the UME content increased the initial value was maintained at approximately 2.8 times than that of neat epoxy.

In the future, it is projected that more diverse lightweight materials and adhesives would be used in automobiles. In this context, the semi-IPN structure demonstrates its effectiveness in addressing the challenges posed by CTE mismatch. Additionally, it offers excellent mechanical properties, making it suitable for application across various fields.

CRedit authorship contribution statement

Kyeng-Bo Sim: Conceptualization, Methodology. **Tae-Hyung Lee:** Conceptualization. **Gi-Yeon Han:** Data curation. **Hyun-Joong Kim:** Supervision.

Declaration of Competing Interest

The authors declare that they have no known competing financial interests or personal relationships that could have appeared to influence the work reported in this paper.

Data availability

Data will be made available on request.

Acknowledgments

This work was supported by the Technology Innovation Program (grant number 20010768, Development of Fast Curing Structural Adhesive with High Performance for Dissimilar Materials on High Speed Process) funded by the Ministry of Trade, Industry & Energy (MOTIE, Korea); World Class 300 Project (R&D) (grant number S2483588) of SMBA (Korea).

Appendix A. Supplementary data

Supplementary data to this article can be found online at <https://doi.org/10.1016/j.compstruct.2023.117426>.

References

- Jin FL, Li X, Park SJ. Synthesis and application of epoxy resins: A review. *J Ind Eng Chem* 2015;29:1–11. <https://doi.org/10.1016/j.jiec.2015.03.026>.
- Hall SA, Howlin BJ, Hamerton I, Baidak A, Billaud C, Ward S. Solving the problem of building models of crosslinked polymers: An example focussing on validation of the properties of crosslinked epoxy resins. *PLoS One* 2012;7. <https://doi.org/10.1371/journal.pone.0042928>.
- Pham HQ, Marks MJ. Epoxy Resins. *Ullmann's Encyclopedia of Industrial Chemistry*, Weinheim, Germany: Wiley-VCH Verlag GmbH & Co. KGaA; 2005. https://doi.org/10.1002/14356007.a09_547.pub2.
- Feng CW, Keong CW, Hsueh YP, Wang YY, Sue HJ. Modeling of long-term creep behavior of structural epoxy adhesives. *Int J Adhes Adhes* 2005;25:427–36. <https://doi.org/10.1016/j.ijadhadh.2004.11.009>.
- Shaw SJ. Adhesives in demanding applications. *Polym Int* 1996;41:193–207. [https://doi.org/10.1002/\(SICI\)1097-0126\(199610\)41:2<193::AID-PI623>3.0.CO;2-6](https://doi.org/10.1002/(SICI)1097-0126(199610)41:2<193::AID-PI623>3.0.CO;2-6).
- Dinu R, Lafont U, Damiano O, Mija A. High Glass Transition Materials from Sustainable Epoxy Resins with Potential Applications in the Aerospace and Space Sectors. *ACS Appl Polym Mater* 2022. <https://doi.org/10.1021/acscapm.2c00183>.
- Wu C, Xu W. Atomistic molecular modelling of crosslinked epoxy resin. *Polymer (Guildf)* 2006;47:6004–9. <https://doi.org/10.1016/j.polymer.2006.06.025>.
- Grant LDR, Adams RD, da Silva LFM. Experimental and numerical analysis of single-lap joints for the automotive industry. *Int J Adhes Adhes* 2009;29:405–13. <https://doi.org/10.1016/j.ijadhadh.2008.09.001>.
- Kinloch AJ, Lee JH, Taylor AC, Sprenger S, Eger C, Egan D. Toughening structural adhesives via nano- and micro-phase inclusions. *J Adhes* 2003;79:867–73. <https://doi.org/10.1080/00218460309551>.
- Suhl D. *Investigations of Large PLCC Package Cracking During Surface Mount Exposure* 1987.
- Chun H, Kim YJ, Tak SY, Park SY, Park SJ, Oh CH. Preparation of ultra-low CTE epoxy composite using the new alkoxyisilyl-functionalized bisphenol A epoxy resin. *Polymer (Guildf)* 2018;135:241–50. <https://doi.org/10.1016/j.polymer.2017.11.048>.
- Kim YJ, Chun H, Park SY, Park SJ, Oh CH. Preparation and curing chemistry of ultra-low CTE epoxy composite based on the newly-designed triethoxysilyl-functionalized ortho-cresol novolac epoxy. *Polymer (Guildf)* 2018;147:81–94. <https://doi.org/10.1016/j.polymer.2018.05.073>.
- El-Tonsy MM. Automatic measurement of the absolute CTE of thin polymer samples: I - Effect of multiple processing on thermal expansion of polypropylene films. *Polym Test* 2004;23:355–60. [https://doi.org/10.1016/S0142-9418\(03\)00102-8](https://doi.org/10.1016/S0142-9418(03)00102-8).
- Choi S, Sankar BV. Gas permeability of various graphite/epoxy composite laminates for cryogenic storage systems. *Compos B Eng* 2008;39:782–91. <https://doi.org/10.1016/j.compositesb.2007.10.010>.
- Roy S, Benjamin M. Modeling of permeation and damage in graphite/epoxy laminates for cryogenic fuel storage. *Compos Sci Technol* 2004;64:2051–65. <https://doi.org/10.1016/j.compscitech.2004.02.014>.
- Boming Z, Zhong Y, Xinyang S. Measurement and analysis of residual stresses in single fiber composite. *Mater Des* 2010;31:1237–41. <https://doi.org/10.1016/j.matdes.2009.09.027>.
- Li T, Zhang J, Wang H, Hu Z, Yu Y. High-performance light-emitting diodes encapsulated with silica-filled epoxy materials. *ACS Appl Mater Interfaces* 2013;5:8968–81. <https://doi.org/10.1021/am402035r>.
- ersoy-varadar-2000-measurement-of-residual-stresses-in-layered-composites-by-compliance-method n.d.
- Bobrov ES, Williamst JEC, Iwasa Y. Experimental and theoretical investigation of mechanical disturbances in epoxy-impregnated superconducting coils. 2. Shear-stress-induced epoxy fracture as the principal source of premature quenches and training-theoretical analysis. 1985.
- Yi JW, Lee YJ, Lee SB, Lee W, Um MK. Effect of dimethylpolysiloxane liquid on the cryogenic tensile strength and thermal contraction behavior of epoxy resins. *Cryogenics (Guildf)* 2014;61:63–9. <https://doi.org/10.1016/j.cryogenics.2014.01.014>.
- Wong CP, Vincent MB, Shi S. *Fast-Flow Underfill Encapsulant: Flow Rate and Coefficient of Thermal Expansion*. vol. 21. 1998.
- Hirata T, Li P, Lei F, Hawkins S, Mullins MJ, Sue HJ. Epoxy nanocomposites with reduced coefficient of thermal expansion. *J Appl Polym Sci* 2019;136. <https://doi.org/10.1002/app.47703>.
- He YX, Sang YF, Zhang L, Yao DH, Sun KB, Zhang YQ. Coefficient of thermal expansion and mechanical properties at cryogenic temperatures of core-shell rubber particle modified epoxy. *Plast, Rubber Compos* 2014;43:89–97. <https://doi.org/10.1179/1743289814Y.0000000074>.
- Chen J, Kinloch AJ, Sprenger S, Taylor AC. The mechanical properties and toughening mechanisms of an epoxy polymer modified with polysiloxane-based core-shell particles. *Polymer (Guildf)* 2013;54:4276–89. <https://doi.org/10.1016/j.polymer.2013.06.009>.
- Park JS, Park SS, Lee S. Thermal and mechanical properties of carbon fiber reinforced epoxy composites modified with CTBN and hydroxyl terminated polyester. *Macromol Symp* 2007;249–250:568–72. <https://doi.org/10.1002/masy.200750438>.
- Kawashita LF, Kinloch AJ, Moore DR, Williams JG. The influence of bond line thickness and peel arm thickness on adhesive fracture toughness of rubber toughened epoxy-aluminium alloy laminates. *Int J Adhes Adhes* 2008;28:199–210. <https://doi.org/10.1016/j.ijadhadh.2007.05.005>.
- Nobelen M, Hayes BS, Seferis JC. Cryogenic Microcracking of Rubber Toughened Composites. *Polym Compos* 2003;24:723–30. <https://doi.org/10.1002/pc.10066>.
- Kim NH, Kim HS. Interaction of toughening mechanisms in a hybrid epoxy system. *J Appl Polym Sci* 2006;100:4470–5. <https://doi.org/10.1002/app.22987>.
- Russell B, Chartoff R. The influence of cure conditions on the morphology and phase distribution in a rubber-modified epoxy resin using scanning electron microscopy and atomic force microscopy. *Polymer (Guildf)* 2005;46:785–98. <https://doi.org/10.1016/j.polymer.2004.11.090>.
- Dean G. Modelling non-linear creep behaviour of an epoxy adhesive. *Int J Adhes Adhes* 2007;27:636–46. <https://doi.org/10.1016/j.ijadhadh.2006.11.004>.
- Lee CC, Lee CC, Chang CP. Simulation methodology development of warpage estimation for epoxy molding compound under considerations of stress relaxation

- characteristics and curing conditions applied in semiconductor packaging. *Mater Sci Semicond Process* 2022;145. <https://doi.org/10.1016/j.mssp.2022.106637>.
- [32] Leguizamón SC, Powers J, Ahn J, Dickens S, Lee S, Jones BH. Polymerization-Induced Phase Separation in Rubber-Toughened Amine-Cured Epoxy Resins: Tuning Morphology from the Nano- To Macro-scale. *Macromolecules* 2021;54:7796–807. <https://doi.org/10.1021/acs.macromol.1c01208>.
- [33] Han IK, Il SK, Jung SM, Jo Y, Kwon J, Chung T, et al. Electroconductive, Adhesive, Non-Swelling, and Viscoelastic Hydrogels for Bioelectronics. *Adv Mater* 2023;35. <https://doi.org/10.1002/adma.202203431>.
- [34] Levita G, De Petris S, Marchetti A, Lazzeri A. Crosslink density and fracture toughness of epoxy resins. n.d.
- [35] Patel A, Mekala S, Kravchenko OG, Yilmaz T, Yuan D, Yue L, et al. Design and Formulation of a Completely Biobased Epoxy Structural Adhesive. *ACS Sustain Chem Eng* 2019;7:16382–91. <https://doi.org/10.1021/acssuschemeng.9b03489>.
- [36] Huang CJ, Fu SY, Zhang YH, Lauke B, Li LF, Ye L. Cryogenic properties of SiO₂/epoxy nanocomposites. *Cryogenics (Guildf)* 2005;45:450–4. <https://doi.org/10.1016/j.cryogenics.2005.03.003>.
- [37] He YX, Li Q, Kuila T, Kim NH, Jiang T, Lau KT, et al. Micro-crack behavior of carbon fiber reinforced thermoplastic modified epoxy composites for cryogenic applications. *Compos B Eng* 2013;44:533–9. <https://doi.org/10.1016/j.compositesb.2012.03.014>.
- [38] Chu X, Huang R, Yang H, Wu Z, Lu J, Zhou Y, et al. The cryogenic thermal expansion and mechanical properties of plasma modified ZrW₂O₈ reinforced epoxy. *Mater Sci Eng A* 2011;528:3367–74. <https://doi.org/10.1016/j.msea.2011.01.003>.
- [39] He Y, Chen Q, Yang S, Lu C, Feng M, Jiang Y, et al. Micro-crack behavior of carbon fiber reinforced Fe₃O₄/graphene oxide modified epoxy composites for cryogenic application. *Compos Part A Appl Sci Manuf* 2018;108:12–22. <https://doi.org/10.1016/j.compositesa.2018.02.014>.
- [40] Zhao H, She W, Shi D, Wu W, Zhang Q, Chao, Li RKY. Polyurethane/POSS nanocomposites for superior hydrophobicity and high ductility. *Compos B Eng* 2019;177. <https://doi.org/10.1016/j.compositesb.2019.107441>.
- [41] Ma C, Qiu S, Wang J, Sheng H, Zhang Y, Hu W, et al. Facile synthesis of a novel hyperbranched poly(urethane-phosphine oxide) as an effective modifier for epoxy resin. *Polym Degrad Stab* 2018;154:157–69. <https://doi.org/10.1016/j.polymdegradstab.2018.05.021>.
- [42] Back JH, Hwang C, Baek D, Kim D, Yu Y, Lee W, et al. Synthesis of urethane-modified aliphatic epoxy using a greenhouse gas for epoxy composites with tunable properties: Toughened polymer, elastomer, and pressure-sensitive adhesive. *Compos B Eng* 2021;222. <https://doi.org/10.1016/j.compositesb.2021.109058>.